

Engineered CRISPR-Base Editors as a Permanent Treatment for Familial Dysautonomia

Supplementary Materials

Supplementary Tables

Attached separately

Supplementary Table 1: GUIDE-seq2 and Cas-OFFinder results

Supplementary Table 2: gRNA target sites

Supplementary Table 3: Plasmids

Supplementary Table 4: Oligonucleotides and probes

Supplementary Table 5: Off-target validation analysis

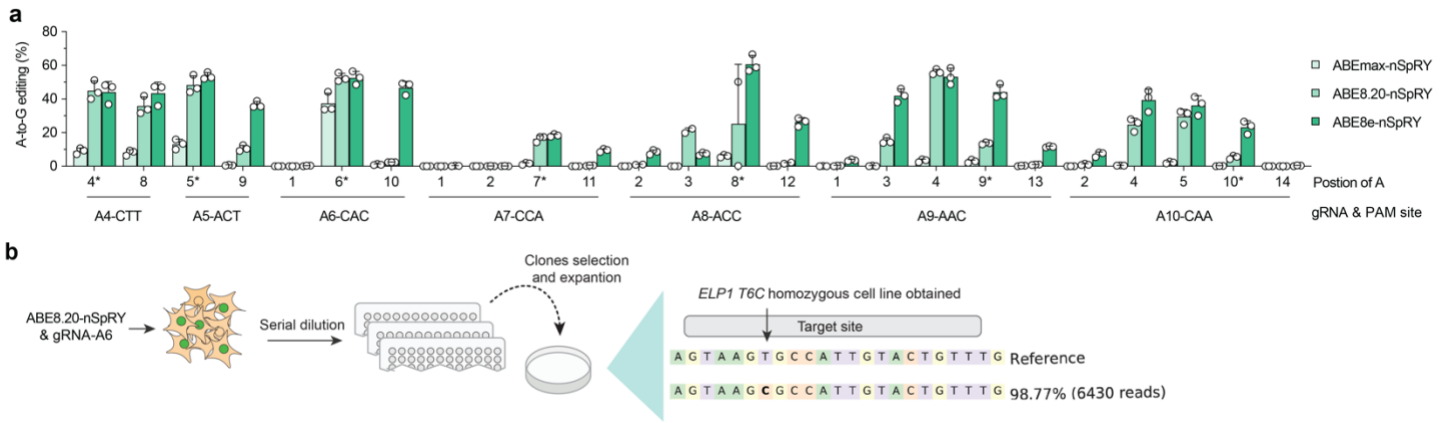
Supplementary Table 6: Primary datasets

NOTE: All Supplementary Tables are attached separately as .xlsx files.

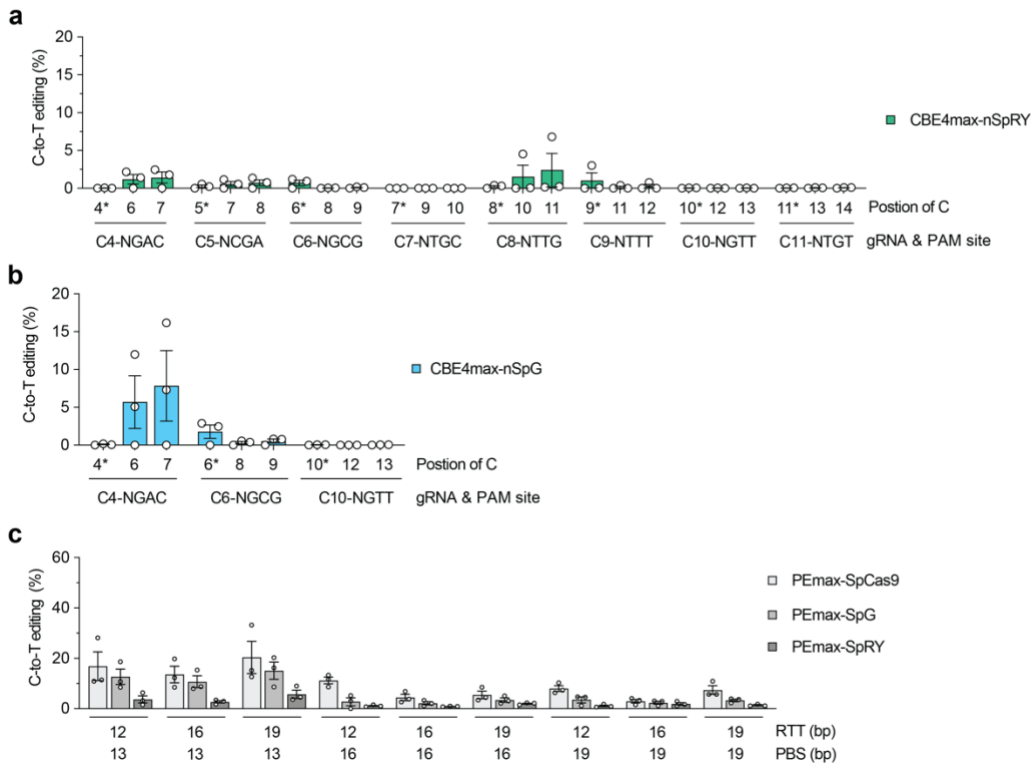
Supplementary Figures and Legends

Supplementary Figures 1-8

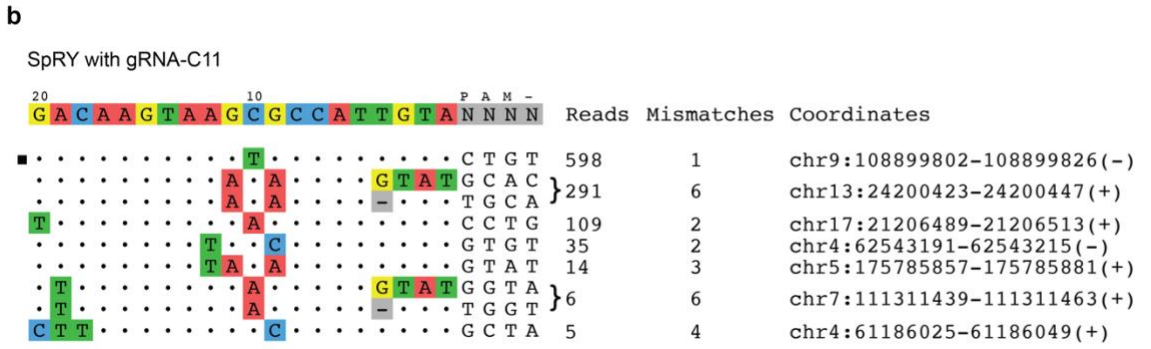
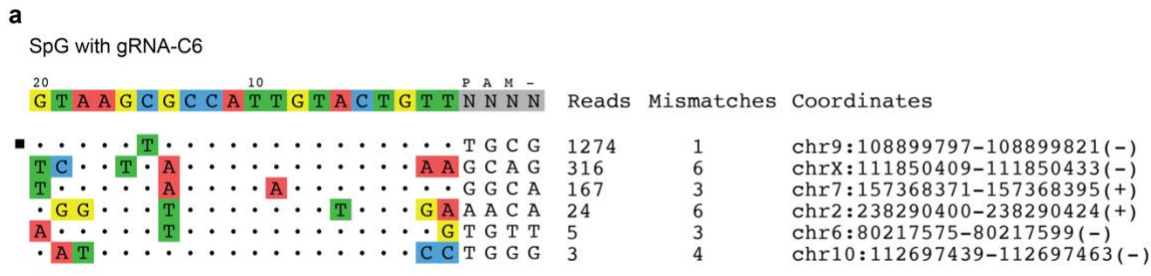
pages 2-9



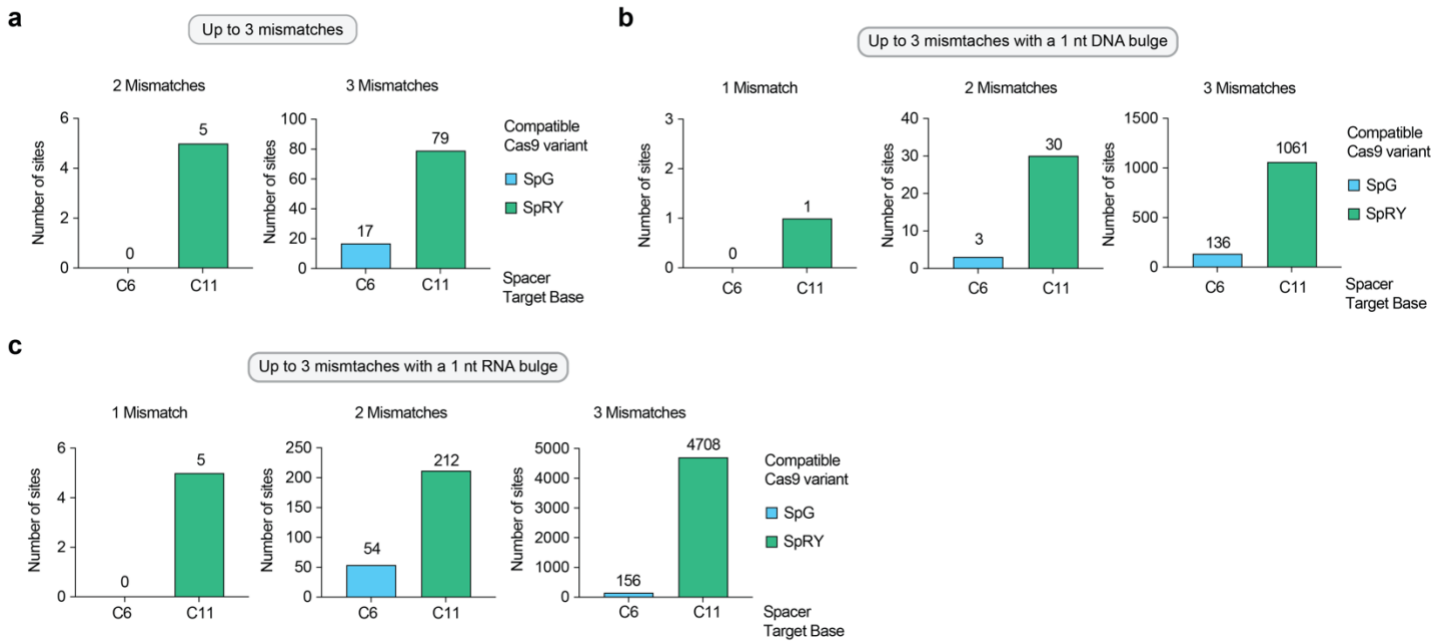
Supplementary Figure 1. Generation of a HEK 293T cell line harboring the *ELP1* T6C mutation via adenine base editing (ABE). **a**, Precise intended A-to-G editing to introduce the *ELP1* T6C mutation using different deaminases fused to the Cas9 variant nSpRY paired with various gRNAs targeting the intended site. Base editing efficiencies assessed by targeted sequencing and analyzed using CRISPResso2; mean, standard errors of the mean (s.e.m.), and individual datapoints shown for n = 3 independent biological replicates. **b**, Schematic of experimental approach to sort and expand clonal HEK 293T cells harboring the *ELP1* T6C mutation when using ABE8.20-nSPRY and gRNA-A6 from **panel a**.



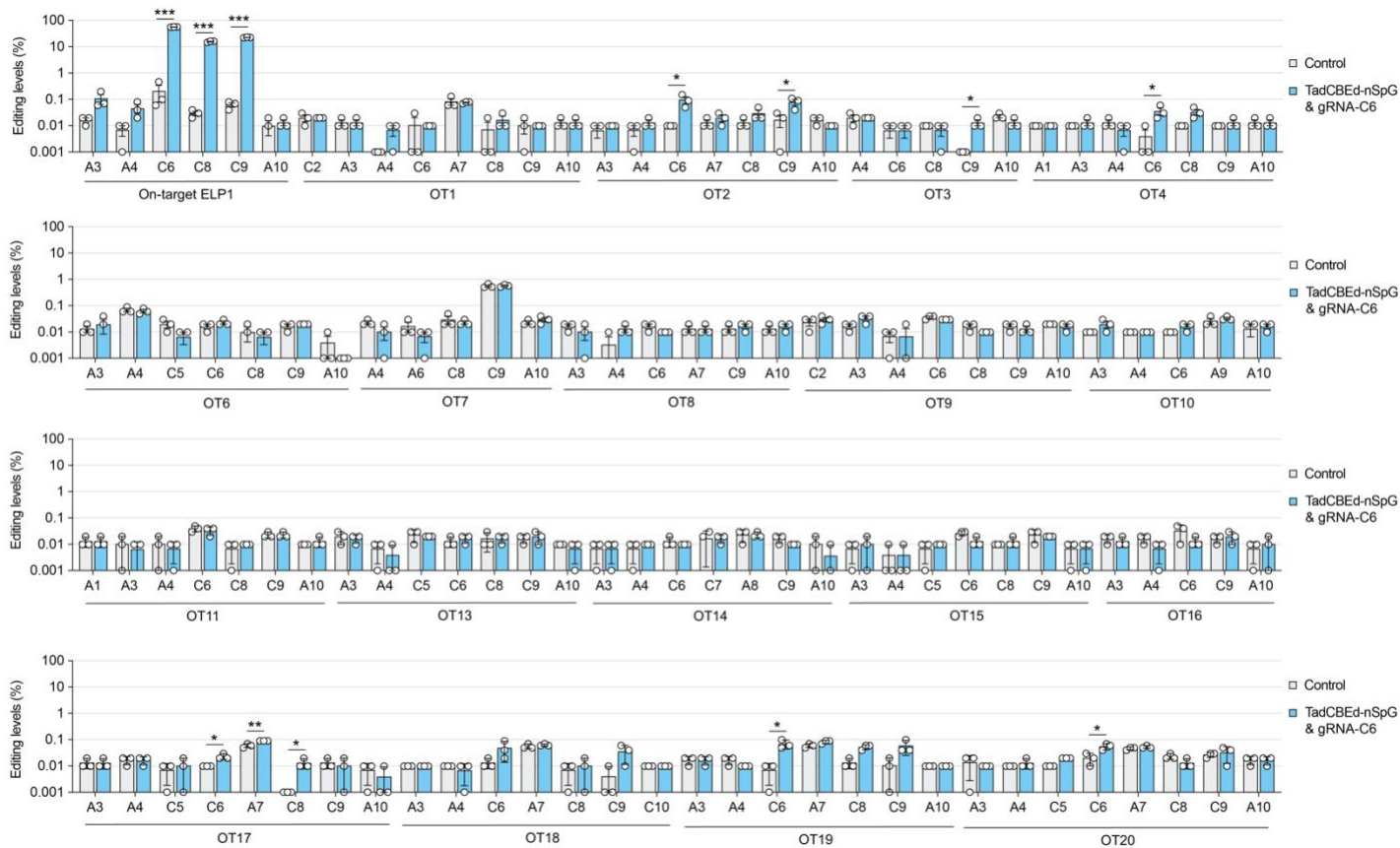
Supplementary Figure 2. Base editing via BE4max or prime editing to correct the *ELP1* T6C mutation. a-b, C-to-T base editing to correct *ELP1* T6C in homozygous HEK293T cells using BE4max, which comprises deaminase domains fused to PAM-variant enzymes SpG and SpRY with gRNA target sites within the editing window. Edited alleles were assessed via targeted sequencing and analyzed using CRISPResso2. c, C-to-T prime editing to precisely correct *ELP1* T6C in homozygous HEK293T cells using PEmax fused with WT SpCas9 and PAM-variant enzymes SpG and SpRY with various combinations of RTT-PBS lengths and a second nicking gRNA targeting the non-targeted strand. Data in **panels a-c are from experiments in HEK293T cells; mean, s.e.m., and individual datapoints shown for n = 3 independent biological replicates.**



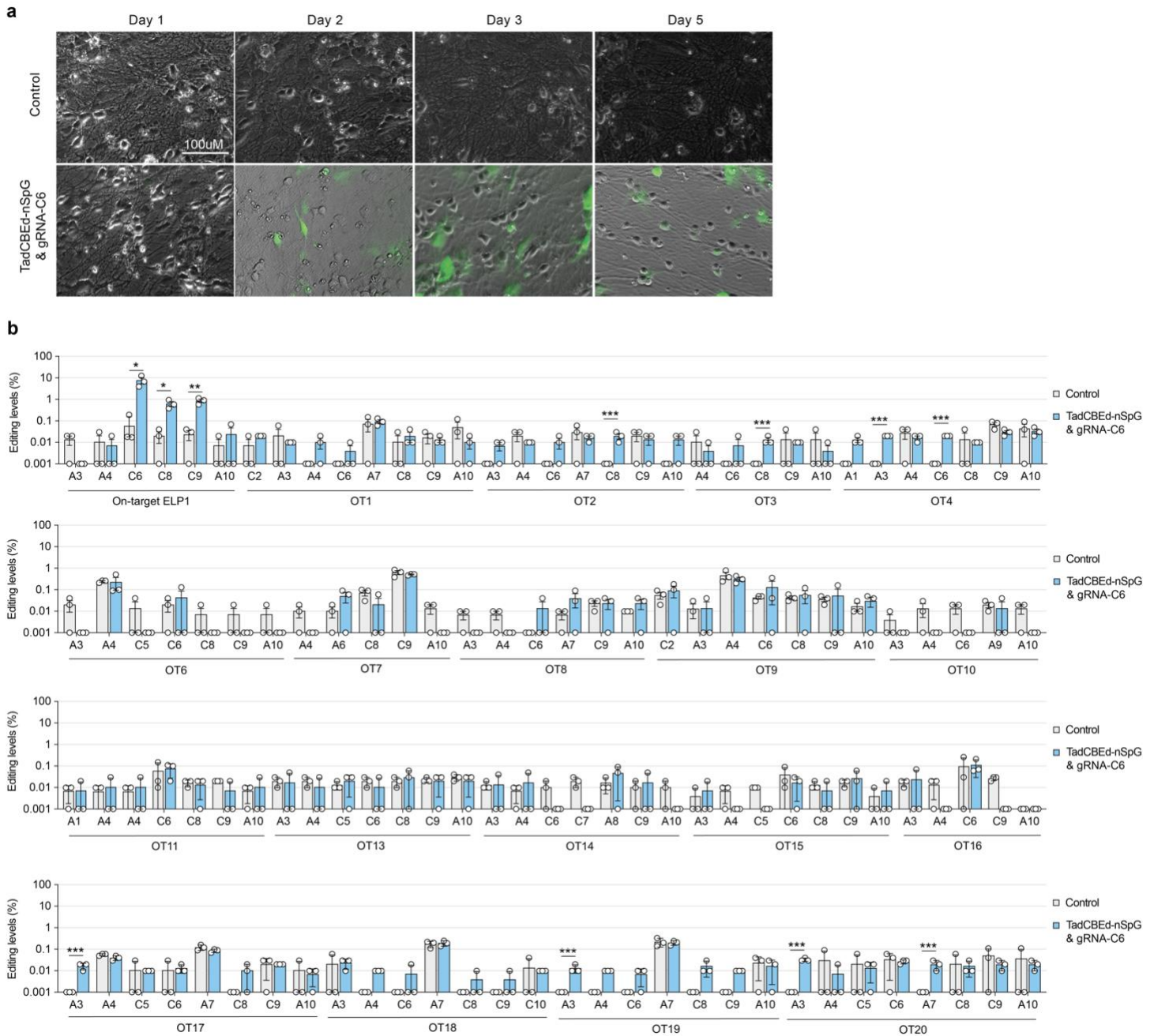
Supplementary Figure 3. Off-target site nomination using the nuclease-based GUIDE-seq2 assay. a-b, Rank-ordered visualization of genomic on- and off-target sites identified by GUIDE-seq2 experiments performed in *ELP1* T6C HEK 293T cells transfected with the SpCas9 variant SpG nuclease and gRNA-C6 (**panel a**), or SpRY nuclease and gRNA-C11 (**panel b**). Mismatched positions in the spacers of the off-target sites are highlighted in color; GUIDE-seq2 read counts from consolidated unique molecular events for each variant are shown to the right of the sequence plots. Datasets represent a single sequencing result from a pool of 3 independent biological replicates prior to sequencing.



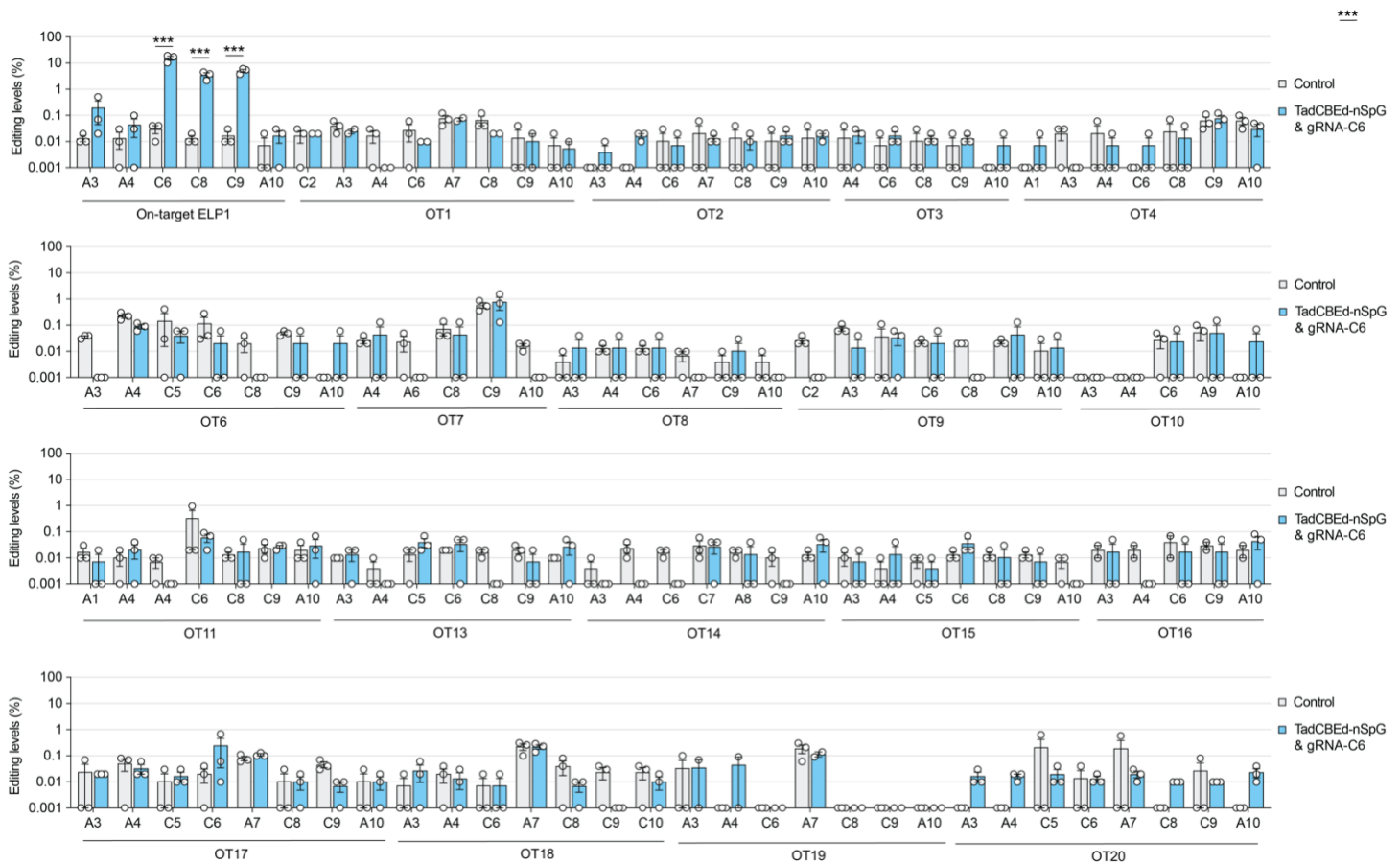
Supplementary Figure 4. *In silico* annotation of putative off-target sites. a-c, Putative off-target sites were identified computationally using CasOFFinder for gRNA C6 with NGN PAM and gRNA C11 with NNN PAM. Off-target sites were nominated when considering up to 3 mismatches (**panel a**), 3 mismatches with a 1 nt DNA bulge (**panel b**), or 3 mismatches with a 1 nt RNA bulge (**panel c**).



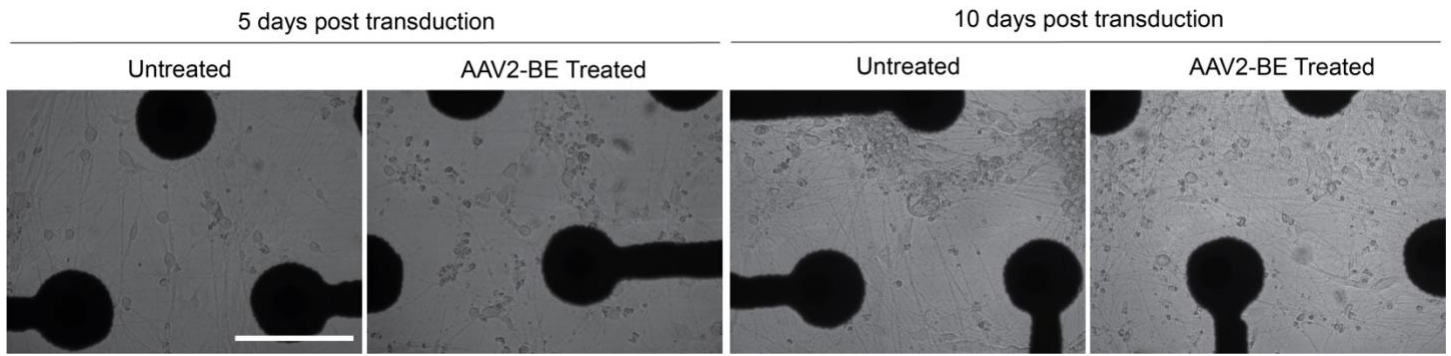
Supplementary Figure 5. Validation of on- and off-target base editing with TadCBEed-nSpG and gRNA C6 in HEK293T-ELP1-TC6 cells. The on-target site and 20 off-target sites were sequenced using PCR and genomic DNA extracted from independent replicates of untreated homozygous HEK293T-ELP1-T6C cells or cells transfected with TadCBEed-SpG and gRNA-C6. Data were analyzed using CRISPResso2, and base editing efficiencies were plotted for all cytosines and adenines (to assess potential bystander A-to-G editing by TadCBEed) across a wide editing window (defined as bases 1–10 within the target site spacer, counting from the PAM-distal end of the spacer). Off-target sites were selected based on all sites nominated by GUIDE-seq2 and those with up to three mismatches identified by CasOFFinder. The genomic regions for off-target sites 5 and 12 failed to amplify or sequence.



Supplementary Figure 6. Validation of on- and off-target base editing with AAV2-EBE in iPSC-derived FD sympathetic neurons. **a**, Bright-field image of untreated iPSC-derived FD sympathetic neurons and GFP fluorescence image of neurons transduced with AAV2-CBE. **b**, On-target site and 20 off-target sites were sequenced using PCR and genomic DNA extracted from independent replicates of untreated samples or samples transduced with AAV2-BE comprised TadCBEd and gRNA-C6. Data were analyzed using CRISPResso2. The base editing efficiencies were plotted for all cytosines and adenines (to assess potential bystander A-to-G editing by CBE) across a wide editing window, defined as bases 1–10 within the target site spacer, counting from the PAM-distal end of the spacer. Off-target sites were selected based on all sites nominated by GUIDE-seq2 and those with up to three mismatches identified by CasOFFinder. The genomic regions for off-target sites 5 and 12 failed to amplify or sequence.



Supplementary Figure 7. Validation of on- and off-target base editing with TadCBE-d-nSpG and gRNA-C6 in FD-fibroblasts. The on-target site and 20 off-target sites were sequenced using PCR and genomic DNA extracted from independent replicates of untreated homozygous human primary fibroblast or transfected with TadCBE-d-nSpG and gRNA-C6. Data were analyzed using CRISPResso2, and base editing efficiencies were plotted for all cytosines and adenines (to assess potential bystander A-to-G editing by CBE) across a wide editing window (defined as bases 1–10 within the target site spacer, counting from the PAM-distal end of the spacer). Off-target sites were selected based on all sites nominated by GUIDE-seq2 and those with up to three mismatches identified by CasOFFinder. The genomic regions for off-target sites 5 and 12 failed to amplify or sequence.



Supplementary Figure 8. Representative images of iPSC-derived FD sympathetic neurons in plates equipped with multielectrode arrays. Representative bright field images of iPSC-derived FD sympathetic neurons untreated or AAV2-BE transduced at day 5 and day 10 post transduction. Scale bar represents 200um.